Novel High Pressure Structures and Superconductivity of $CaLi_2$

Yu Xie,[1,2] Artem R. Oganov,[2,3] and Yanming Ma[1,*]

[1]*State Key Lab of Superhard Materials, Jilin University, Changchun 130012, China*

[2]*Department of Geosciences, Department of Physics and Astronomy, and New York Center for Computational Science, Stony Brook University, Stony Brook, New York 11794-2100, USA*

[3]*Department of Geology, Moscow State University, 119992 Moscow, Russia*

(Received 29 January 2010; published 29 April 2010)

Using evolutionary methodology for crystal structure prediction, we explore high-pressure phases of $CaLi_2$, a compound made of two elements that show anomalies upon compression. In addition to the known low-pressure Laves phases, we find two novel structures with space groups $C2/c$ and $P2_1/c$, stable at pressure ranges of 35–54 GPa and 54–105 GPa, respectively. It is found that decomposition into pure elements is energetically favorable at pressures of 20–35 GPa and above 105 GPa. Such decomposition-recombination-decomposition oscillating behavior with pressure is predicted for the first time in a binary compound. The $C2/c$ and $P2_1/c$ phases are predicted to be superconductors, and the calculated T_c of $\sim$15 K at 45 GPa is in good agreement with experiment.

DOI: 10.1103/PhysRevLett.104.177005 PACS numbers: 74.70.Ad, 71.20.Lp, 74.25.−q, 74.62.Fj

High-pressure behavior of metals is of great importance to planetary physics and materials science. Recent studies show that simple s, p metals, such as Li, Na, and Ca, exhibit anomalous properties under compression, e.g., enhanced superconductivity [1–3], strong increase of the electrical resistivity [3–5], valence bandwidth narrowing [6–8], and metal-to-semiconductor transition [5,9]. These behaviors are in contrast to the expected tendency towards free-electron-like behavior under pressure. It is suggested [6,7,9] that such anomalies can arise from the increased localization of valence electrons as they are excluded from the ionic core regions and trapped into interstitial regions. These arguments are quite general and the underlying effects can exist in other elements and compounds under sufficient compression [7]. $CaLi_2$, the only binary compound formed by Li and Ca, is one of the simplest compounds for testing these ideas.

Feng *et al.* [10] carried out electronic structure calculations for hexagonal ($MgZn_2$ type) and cubic ($MgCu_2$ type) Laves phases of $CaLi_2$ and suggested that the hexagonal symmetry of $CaLi_2$ is stable up to over 200 GPa but undergoes a significant lattice bifurcation around 47 GPa. It was also predicted that $CaLi_2$ could be a potential superconductor under pressure due to the high density of states at Fermi level, the high dynamical scale of Li, and the favorable interlayer phonons. Superconductivity was subsequently observed in $CaLi_2$ at pressures above 11 GPa [11] with a maximum T_c of 13 K near 40 GPa. Debessai *et al.* [12] measured the x-ray diffraction patterns of $CaLi_2$ up to 54 GPa and found that hexagonal Laves-type $CaLi_2$ undergoes a phase transition above 23 GPa and completely transforms into an orthorhombic phase at 46 GPa. However, Tse *et al.* [13] proposed that $CaLi_2$ becomes unstable against decomposition into Ca and Li at high pressure, and thus the superconductivity measurements are contaminated by elemental Ca and Li.

The peculiarity of $CaLi_2$, together with the significant discrepancy between previous works, motivates the present study. Here, we performed an extensive search for stable high-pressure crystal structures of $CaLi_2$ using an evolutionary structure prediction algorithm. Simulations uncovered two novel structures, with space groups $C2/c$ and $P2_1/c$, to be stable at pressure ranges of 35–54 GPa and 54–105 GPa, respectively. Intriguingly, the computed thermodynamics suggest that $CaLi_2$ is stable in the hexagonal Laves phase below 20 GPa, decomposes in the pressure range of 20–35 GPa, and then restabilizes before the final decomposition into elemental Ca and Li above 105 GPa. Furthermore, the calculated T_c is in good agreement with experimental measurements. Our results suggest that the measured superconductivity [11] is from the $CaLi_2$ compound, and is not contaminated by decomposition into the elements.

Structure searches for $CaLi_2$ were performed with the *ab initio* evolutionary algorithm USPEX [14–16]. This approach has been successfully used in a number of other applications (e.g., Refs. [9,17–19]). The underlying *ab initio* structural relaxations and electronic properties calculations were carried out using density functional theory [20,21] within the PBE exchange-correlation [22] as implemented in the VASP code [23]. The all-electron projector-augmented wave method [24] was adopted with $1s^2 2s^1$ and $3s^2 3p^6 4s^2$ treated as valence electrons for Li and Ca, respectively. Lattice dynamics and electron-phonon coupling were performed with the QUANTUM-ESPRESSO package [25,26].

We have performed structure prediction simulations in the pressure range of 10–250 GPa within 20 or 30 GPa interval with 1, 2, 3, 4, 6, and 8 f.u. in the simulation cells. In the low-pressure range of 10–20 GPa, we found the hexagonal Laves phase as the most stable structure, in agreement with experiment. At higher pressure, besides

the previously predicted $I4_1/amd$ and $I2_12_12_1$ structures [10], we uncovered a group of new structures. Among them, the monoclinic structures $C2/c$ and $P2_1/c$ were found to be stable at certain pressure ranges. The two predicted structures are interesting, as they show Li-Li paring [6], the well-known $ThSi_2$ [27], and graphene motifs. At 36 GPa, the $C2/c$ structure [Fig. 1(a)] is ~5% denser than the hexagonal Laves phase, and has Ca atoms forming topologically the same (save for a symmetry-breaking distortion) arrangement as the Si-sublattice in α-$ThSi_2$ [27], a known superconductor. The two inequivalent Li atoms form Li_2 pairs, stuffing the Ca framework. Contrary to the three-dimensional $C2/c$ structure, the $P2_1/c$ structure [Figs. 1(a)–1(d)] has a flavor of 2D geometry. The structure can be viewed as a slight distortion of a trigonal P-$3m1$ structure [26] or a strong distortion of a hexagonal $P6/mmm$ structure [26]. The Ca and Li2 atoms form alternating graphene layers stacked on top of each other; Li1 atoms adopt linear chains running through centers of hexagonal channels [Fig. 1(b)]. In a recent experimental study [12], indexing of the powder diffraction pattern gave an orthorhombic unit cell (but the atomic positions were not determined), and that cell is close to our calculation for the $P2_1/c$ structure—except that our cell is monoclinic (with the β-angle of 90.028°, very close to the "orthorhombic" 90°) [26]. Note that there is a moderate volume overexpansion in theory, typical of GGA calculations. An additional structure search at the fixed experimental unit cell produced the same $P2_1/c$ structure.

The enthalpy difference curves (relative to decomposition into pure elements) [19,28] as a function of pressure for various structures are presented in Fig. 2(a). The structures we find here are clearly superior to the previously predicted structures. The pressure evolution of $CaLi_2$ is quite surprising. Below 20 GPa, the hexagonal Laves-type

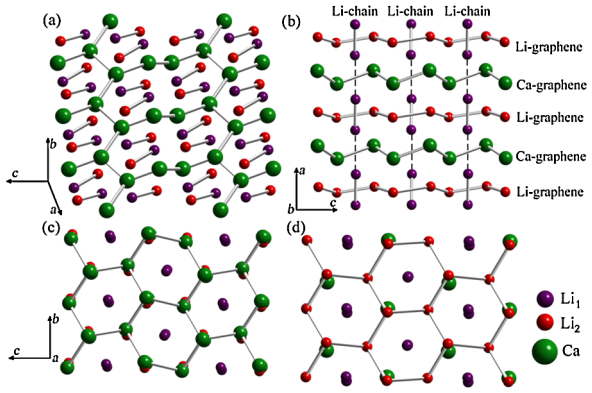

FIG. 1 (color online). The most stable structures found in evolutionary simulations at (a) 36 GPa ($C2/c$ structure) showing the connectivity of the Ca-sublattice and Li1 and Li2 paring, and (b)–(d) the $P2_1/c$ structure at 55 GPa. (b) Stacking of distorted Ca and Li2 graphene sheets and Li1 linear chains, (c) Ca and (d) Li2 sublattice. Detailed structural information is given in the supplementary information [26].

structure is stable, at pressures 20–35 GPa decomposition into the elements becomes favorable, then $C2/c$ (35–54 GPa) and $P2_1/c$ (54–105 GPa) structures take over, and finally $CaLi_2$ decomposes again above 105 GPa. Such oscillatory decomposition-recombination-decomposition behavior is known, for instance, for $MgAl_2O_4$ [29], but to our knowledge, this is the first report of such phenomenon for a binary compound. The solid-state reactions, such as decomposition and recombination, usually have high activation energies, and thus a high temperature experiment might be necessary to conquer the kinetic barrier of the decomposition/recombination of $CaLi_2$ as suggested also in Ref. [13].

The evolution of the density of states (DOS) at Fermi level (N_F) and the valence bandwidth as a function of pressure is presented in Fig. 2(b). It is clear that after an initial increase, the valence bandwidth decreases with pressure, a behavior similar to what has been found in the "exotic" high-pressure metals Li [6], Na [7], and Ca [8]. N_F rises as pressure increases to 10 GPa, then drops dramatically as a deep pseudogap. Moreover, N_F has a dramatic increase at the transition into the $P2_1/c$ phase. This is probably related to the peculiar 2D geometry of the $P2_1/c$ structure. By examining the band structure, we found that there are two extra bands crossing the Fermi level in the $P2_1/c$ structure compared to $C2/c$ [26]. Thus, a small peak emerges at the Fermi level, and the DOS at the Fermi level increases. Contrary to what was predicted in Ref. [10], we found that N_F decreases in a wide pressure range [Fig. 2(b)]. This behavior arises from localization of the valence electrons in the interstices of the structure, as they are pushed away from the ionic cores [7,9], a phenomenon related to the core-valence repulsion at high pressure. The shortest Li-Li, Li-Ca, and Ca-Ca distances in the $P2_1/c$ structure at 100 GPa are 1.60, 1.90, and 2.26 Å, respectively, which implies strong core-valence interaction between neighboring atoms (the ionic radii of Ca and Li, measuring spatial extent of their cores, are 1.0 and 0.76 Å, while the 2s-orbital radius for Li is 1.62 Å and the 4s-orbital radius for Ca is 1.69 Å). Figures 2(c)–2(e) show the unusual distribution of the valence electron localization function (ELF) of $P2_1/c$ structure at 100 GPa; it has maxima not only at the nuclei, but also in the interstices. These results are consistent with the experimental observation [12] of a sharp increase of the electrical resistivity upon compression.

Phonon calculations did not show any imaginary frequencies, indicating dynamical stability of both $C2/c$ and $P2_1/c$ structures (Fig. 3). From the phonon band structure and the site-projected phonon DOS (Fig. 3), it is found that at 36 GPa, the low-energy phonon modes (0–225 cm^{-1}) are mainly associated with Ca atoms due to their much higher atomic mass. The intermediate frequencies (225–320 cm^{-1}) correspond to the coupled Ca-Li vibrations, while above 320 cm^{-1}, the Li-Li vibrations dominate. We found several interesting phonon features under pressure [26]. For the $C2/c$ phase, all phonons harden up to

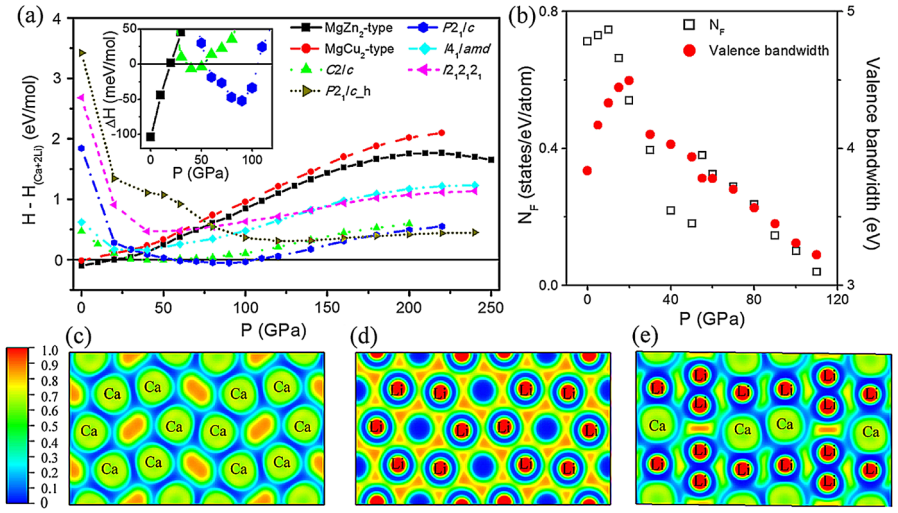

FIG. 2 (color online). (a) Enthalpy curves (with respect to the mixture of the elements) of various $CaLi_2$ structures. Enthalpies are given per formula unit. Inset: Enthalpies of the hexagonal Laves type, $C2/c$, and $P2_1/c$ structures shown on a different scale for clarity. (b) Evolution of the valence bandwidth and N_F as a function of pressure. (c)–(e) Valence ELF of $P2_1/c$ structure at 100 GPa. (c) and (d) The (100) sections through the middle of Ca and Li2 graphene layer, respectively. (e) The (010) section through Li1 linear chains. The ELF peaks are located at nuclei (core orbitals) and in the interstices (valence electrons that are excluded from the core regions).

36 GPa, then the transverse acoustic (TA) modes along the A-M-Y and V-L-Γ directions and two optical modes B_u (242 cm^{-1}) and B_g (279 cm^{-1}) along the V-L-Γ direction soften, while rise again above 45 GPa. It is also found that the A_g mode near the Γ point and TA modes along the Z-C-Y direction are very low in the $P2_1/c$ structure at 60 GPa. At higher pressure, these modes harden, but the frequencies of TA modes along the E-D-Γ direction begin to drop. At 100 GPa, the optical A_u mode becomes ultrasoft near the Γ point with a very small frequency of 18 cm^{-1}.

The electron-phonon coupling (EPC) calculations have been performed to explore the superconductivity. The Eliashberg phonon spectral function $\alpha^2F(\omega)/\omega$, logarithmic average phonon frequency $\omega_{\log}$, and the EPC strength λ as a function of pressure are shown in Fig. 4. The superconducting T_c has been estimated from the Allen-

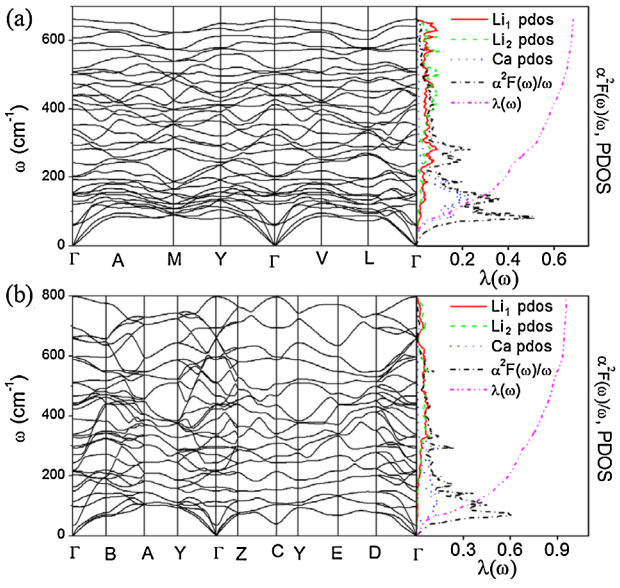

FIG. 3 (color online). (a) and (b) Phonon dispersion, Eliashberg phonon spectral function, and site-projected phonon DOS of $C2/c$ and $P2_1/c$ structures at 36 and 60 GPa, respectively.

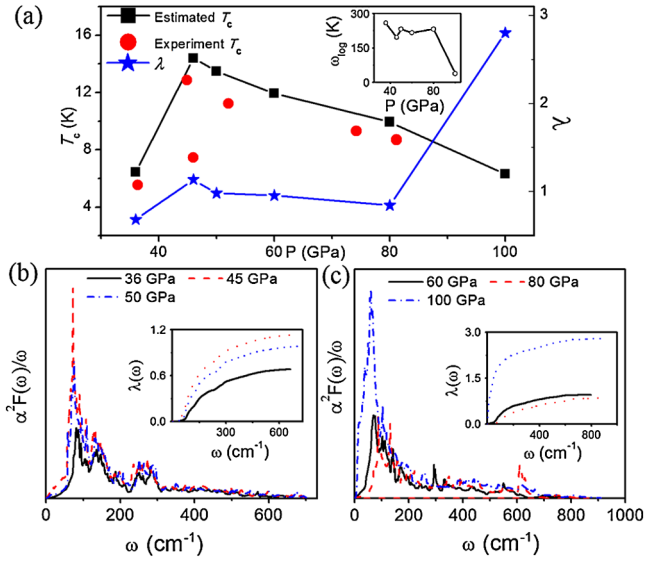

FIG. 4 (color online). (a) Pressure dependence of T_c and λ. The inset shows the evolution of the logarithmic average phonon frequency with pressure. (b) and (c) The spectral function $\alpha^2F(\omega)/\omega$ at selected pressures for $C2/c$ and $P2_1/c$ phases, respectively. The electron-phonon coupling integral $\lambda(\omega)$ is plotted in the inset.

Dynes modified McMilan equation [30], and a typical value of Coulomb pseudopotential $\mu^* = 0.13$ is used. The predicted T_c is in a very good agreement with experimental results [Fig. 4(a)]. According to the McMilan equation, T_c is dominated by $\omega_{\log}$, λ, and N_F. N_F is less important, being small and decreasing upon compression. The λ and $\omega_{\log}$ are more critical for T_c, and one observes that λ and $\omega_{\log}$ have an almost opposite evolution with pressure [Fig. 4(a)]. Both of them can be derived from $\alpha^2F(\omega)/\omega$ [30]. Moreover, the evolution of the spectral function is a reflection of the phonon behaviors. Obviously, the low-frequency Ca vibrations in $C2/c$ phase at 36 GPa are the main contributors to the spectral function with a pronounced peak at 70–225 cm^{-1}. Nearly 70% of λ originates from this frequency range. As pressure increases, the peak shifts to lower frequency and becomes much stronger at 45 GPa, where phonon softening is most severe. This comes with a 24% reduced $\omega_{\log}$ from 259 to 196 K. It is noteworthy that the partial coupling strengths $\lambda_{q\nu}$ of the softening modes are enhanced in inverse proportion to $\omega_{q\nu}$, resulting in a notable increase of λ from 0.68 to 1.14 (66%) (Fig. 4, [26]), leading to a high $T_c \sim 15$ K. Above 45 GPa, phonon frequencies harden, and a reverse behavior is seen [Fig. 4(b)], resulting in a decreased λ in spite of the increased $\omega_{\log}$, and a lowering of T_c is also observed. Similar behavior is also found in the $P2_1/c$ phase. The correlation between superconducting T_c and phonon softening/hardening is remarkably clear here. We therefore conclude that the high-pressure superconductivity is mainly related to the low-energy Ca modes rather than the high-frequency Li vibrations predicted in [10].

In summary, we found two novel high-pressure structures of $CaLi_2$, $C2/c$, and $P2_1/c$, which are stable in pressure ranges of 35–54 GPa and 54–105 GPa, respectively. These phases possess intriguing crystal structures and peculiar superconductivity under pressure. A decomposition-recombination-decomposition phenomenon is predicted for the first time in a binary compound. The observed sharp increase of electrical resistivity in $CaLi_2$ under high pressure can be attributed to the localization of valence electrons in the interstices of the lattice, at the roots of which is the core—valence overlap between neighboring atoms. Our electron-phonon coupling calculations confirm that the high-pressure superconductivity of $CaLi_2$ arises from the compound itself, but not the elements Ca and Li. The calculated T_c matches well with the experimental results; the main contributions to superconductivity arise from the low-frequency Ca vibrations and T_c is dominated by the phonon softening/hardening. Our predictions can be verified in future experiments by performing simultaneous measurements of superconductivity and x-ray diffraction under pressure.

The authors acknowledge funding from the National Natural Science Foundation of China (NSFC) under Grants No. 10874054, the NSFC awarded Research Fellowship for International Young Scientists under Grant No. 10910263, Jilin University (No. 200905003), and the 2007 Cheung Kong Scholars Program of China, the Research Foundation of Stony Brook University, Intel Corporation, and Rosnauka (Russia, Contract No. 02.740.11.5102). Calculations were performed on the NYBlue supercomputer (NYCCS), on the Skif MSU supercomputer (Moscow State University, Russia), and at the Joint Supercomputer Center (Russian Academy of Sciences).

*Corresponding author: mym@jlu.edu.cn

[1] K. Shimizu *et al.*, Nature (London) **419**, 597 (2002).
[2] V. V. Struzhkin *et al.*, Science **298**, 1213 (2002).
[3] T. Yabuuchi *et al.*, J. Phys. Soc. Jpn. **75**, 083703 (2006).
[4] T. H. Lin and K. J. Dunn, Phys. Rev. B **33**, 807 (1986).
[5] T. Matsuoka and K. Shimizu, Nature (London) **458**, 186 (2009).
[6] J. B. Neaton and N. W. Ashcroft, Nature (London) **400**, 141 (1999).
[7] J. B. Neaton and N. W. Ashcroft, Phys. Rev. Lett. **86**, 2830 (2001).
[8] S. Lei, D. A. Papaconstantopoulos, and M. J. Mehl, Phys. Rev. B **75**, 024512 (2007).
[9] Y. M. Ma *et al.*, Nature (London) **458**, 182 (2009).
[10] J. Feng, N. W. Ashcroft, and R. Hoffmann, Phys. Rev. Lett. **98**, 247002 (2007).
[11] T. Matsuoka *et al.*, Phys. Rev. Lett. **100**, 197003 (2008).
[12] M. Debessai *et al.*, Phys. Rev. B **78**, 214517 (2008).
[13] J. S. Tse *et al.*, Europhys. Lett. **86**, 56001 (2009).
[14] A. R. Oganov and C. W. Glass, J. Chem. Phys. **124**, 244704 (2006).
[15] A. R. Oganov, C. W. Glass, and S. Ono, Earth Planet. Sci. Lett. **241**, 95 (2006).
[16] C. W. Glass, A. R. Oganov, and N. Hansen, Comput. Phys. Commun. **175**, 713 (2006).
[17] A. R. Oganov *et al.*, Nature (London) **457**, 863 (2009).
[18] Y. M. Ma, A. R. Oganov, and Y. Xie, Phys. Rev. B **78**, 014102 (2008).
[19] A. R. Organov *et al.*, Proc. Natl. Acad. Sci. (to be published).
[20] P. Hohenberg and W. Kohn, Phys. Rev. **136**, B864 (1964).
[21] W. Kohn and L. J. Sham, Phys. Rev. **140**, A1133 (1965).
[22] J. P. Perdew, K. Burke, and M. Ernzerhof, Phys. Rev. Lett. **77**, 3865 (1996).
[23] G. Kresse and J. Furthmuller, Phys. Rev. B **54**, 11169 (1996).
[24] P. E. Blöchl, Phys. Rev. B **50**, 17953 (1994).
[25] S. Baroni *et al.*, http://www.pwscf.org/.
[26] See supplementary material at http://link.aps.org/supplemental/10.1103/PhysRevLett.104.177005 for additional high pressure structural, electronic, and dynamical properties.
[27] K. Klepp and E. Parthé, Acta Crystallogr. Sect. B **38**, 1105 (1982).
[28] Y. S. Yao , J. S. Tse, and D. D. Klug, Phys. Rev. Lett. **102**, 115503 (2009).
[29] T. Irifune, K. Fujino, and E. Ohtani, Nature (London) **349**, 409 (1991).
[30] P. B. Allen and R. C. Dynes, Phys. Rev. B **12**, 905 (1975).